Universiteit
Leiden
The Netherlands

The role of autophagy during carbon starvation in Aspergillus niger

Burggraaf, M.A.

Citation
Burggraaf, M. A. (2021, May 25). *The role of autophagy during carbon starvation in Aspergillus niger*. Retrieved from https://hdl.handle.net/1887/3179455

Version:	Publisher's Version
License:	Licence agreement concerning inclusion of doctoral thesis in the Institutional Repository of the University of Leiden
Downloaded from:	https://hdl.handle.net/1887/3179455

Note: To cite this publication please use the final published version (if applicable).

Cover Page

Universiteit Leiden

The handle https://hdl.handle.net/1887/3179455 holds various files of this Leiden University dissertation.

Author: Burggraaf, M.A.
Title: The role of autophagy during carbon starvation in Aspergillus niger
Issue Date: 2021-05-25

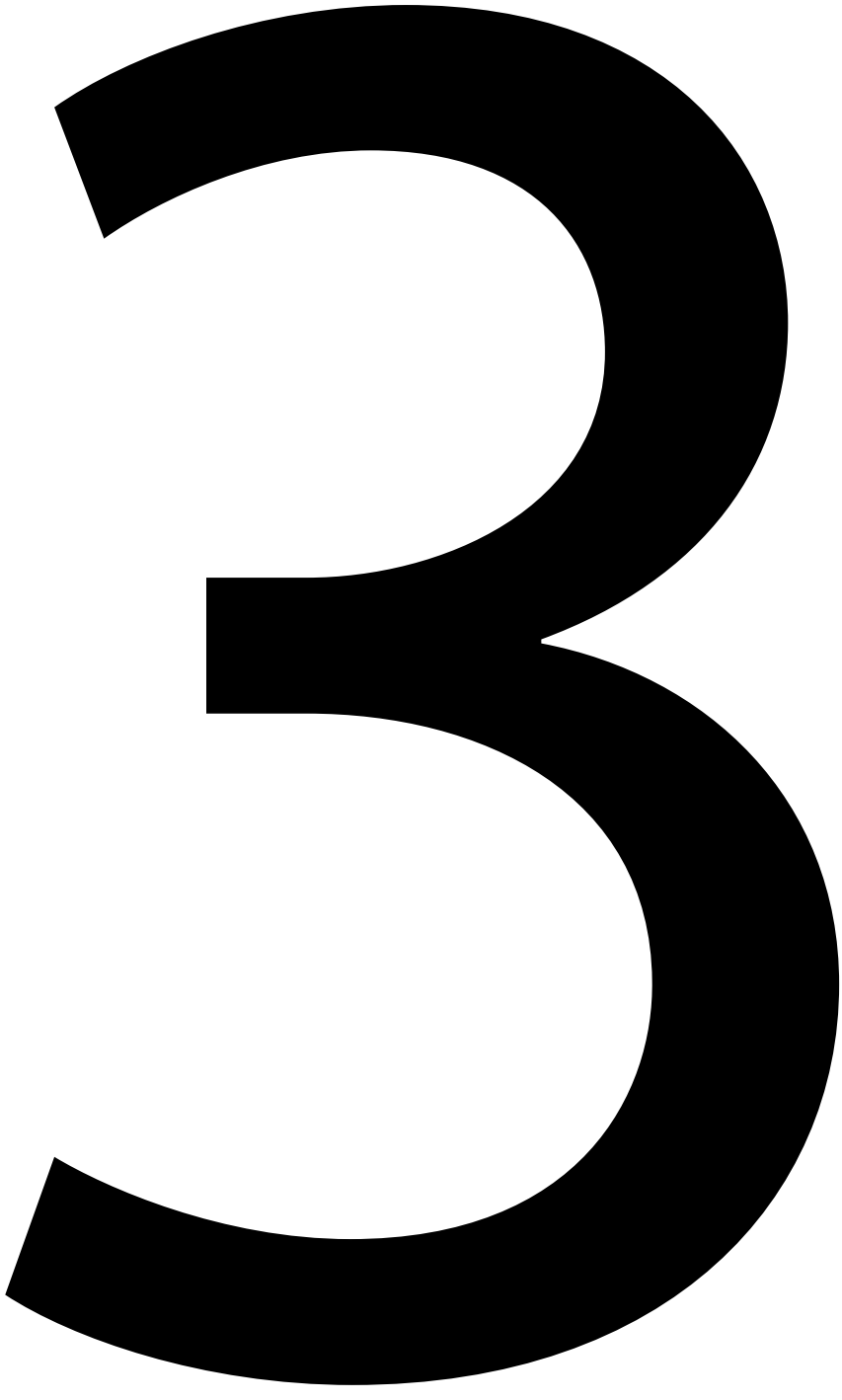

Chapter 3

Transcriptional profiling of the *Aspergillus niger* Δ*atg1* mutant during submerged carbon starvation

Anne-Marie Burggraaf[1], Cees A.M.J.J. van den Hondel[1], Peter J. Punt[2] and Arthur F.J. Ram[1]

[1] Leiden University, Institute of Biology Leiden, Molecular Microbiology and Biotechnology, Sylviusweg 72, 2333 BE Leiden, The Netherlands

[2] Dutch DNA Biotech, Hugo R Kruytgebouw 4-Noord, Padualaan 8, 3584 CH Utrecht, The Netherlands.

Abstract

During limitations in the available nutrient sources, *Aspergillus niger* modifies the expression of specific sets of genes in order to respond to these stress conditions. Among them, autophagy-related (*atg*) genes are concertedly induced. Autophagy is a catabolic process during which organelles and cellular content are delivered to vacuoles for degradation and recycling. Deleting genes essential for autophagy hardly affected growth during the exponential phase, but the mutants did show morphological deviations during submerged carbon starvation as the formation of thin hyphae was accelerated in comparison with the wild-type. This present study aimed to obtain more insight in the underlying processes causing these changes by performing genome-wide transcriptional analysis comparing the *A. niger* Δ*atg1* mutant with the wild-type during submerged carbon starvation. Gene enrichment analysis demonstrated that in the *Δatg1* mutant bioprocesses related to DNA repair and cell division were higher expressed during the early post-exponential phase compared to the wild-type strain while at the later starvation time points ribosomal genes as well as metabolic processes showed lower expression. The data further support that autophagy is important during carbon starvation in order to control cell cycle arrest, degrade harmful cellular components and to support morphological and metabolic changes by endogenous recycling.

Introduction

Filamentous fungi with a saprophytic lifestyle, such as *Aspergillus niger* commonly encounter limitations in the available exogenous carbon source when growing in their natural environment. In response to such conditions, specific processes are induced leading to complex morphological and physiological changes which help the fungus to adapt to starvation stress. Important aspects of the carbon starvation response include the recycling of nutrients and the formation of asexual spores (Nitsche *et al.*, 2012; Szilágyi *et al.*, 2013; Ellström *et al.*, 2015; van Munster *et al.*, 2015b). Genome-wide transcriptomics studies have revealed that autophagy is one of the most dominantly induced processes upon starvation conditions in filamentous fungi (Nitsche *et al.*, 2012; Krohn *et al.*, 2014), which indicates that recycling of cell contents via autophagy plays an important role in order to survive nutrient limitation conditions. The autophagy process involves sequestering of cellular components in double membrane vesicles, which fuse with vacuoles releasing their contents for degradation by hydrolytic enzymes. The autophagy machinery is negatively regulated by the target of rapamycin (Tor) and the protein kinase A (PKA), which sense the nutritional state of a cell and inactivate the autophagy-related protein 13 (Atg13) during nutrient-rich conditions by phosphorylation. During starvation conditions, Atg13 is able to interact with Atg1 to form the Atg1 kinase complex, which initiates the autophagy process (Kamada *et al.*, 2000; Stephan *et al.*, 2009).

The (endogenous) recycling of nutrients by autophagy is important for maintenance of the mycelium, but also to fuel asexual development and cellular differentiation. Both in *A. niger* and *A. oryzae* it has been shown that carbon recycling fuels the secondary growth of hyphae with decreased hyphal diameters on the expense of older hyphal compartments, which become empty (Pollack *et al.*, 2008; Nitsche *et al.*, 2012). As the deletion of genes essential for autophagy accelerated the relative abundance of thin (young) hyphae in comparison with thick (old) compartments during submerged carbon starvation (Nitsche *et al.*, 2013), it has been proposed that autophagy protects older hyphae from cell death, balancing between survival of the mycelium and the formation of foraging hyphae. Studying of autophagy mutants further showed that deletion of autophagy-essential genes affected conidiation in a number of *Aspergilli* (Kikuma *et al.*, 2006; Richie *et al.*, 2007; Kikuma and Kitamoto, 2011; Nitsche *et al.*, 2013; Pinar *et al.*, 2013), although the effects varied between a mild reduction in sporulation in *A. fumigatus* and *A. niger* to a complete impairment of formation of aerial hyphae and conidia in *A. oryzae*.

To gain more insights in the underlying processes driving starvation-induced physiological and morphological changes, we performed genome-wide transcriptional analyses of glucose-starved submerged cultures of *A. niger* wild-type and Δ*atg1* strains using RNA sequencing. Gene expression of wild-type and mutant was compared during the

exponential growth phase and three carbon starvation time points, and enrichment analysis was performed to interpret the complex transcriptional changes. The results showed that after one day of carbon starvation the expression of genes related to cell division and DNA repair was higher in the Δ*atg1* mutant compared to the wild-type. Furthermore, protein synthesis and metabolic processes were significantly lower in the Δ*atg1* mutant during the later stages of carbon starvation. Taken together, the data suggest that the autophagy process plays an important role in order to support cellular integrity and metabolic adaptation during nutrient-limited conditions.

Materials and Methods

Cultivation, RNA isolation and quality control

Duplicate bioreactor batch cultivations of *A. niger* wild-type (N402) and Δ*atg1* (BN30.2) strains under prolonged carbon starvation conditions were performed and described previously (Nitsche *et al.*, 2013). Mycelium intended for gene expression analysis was separated from culture medium and frozen in liquid nitrogen within 15-20 s from sampling and stored at -80°C. Total RNA was extracted from mycelium in liquid nitrogen using Trizol reagent (Invitrogen). Frozen ground mycelium (≈200 mg) was directly suspended in 800 µl Trizol reagent and vortexed vigorously for 1 min. After 5 min of incubation at room temperature, 150 µl of chloroform was added. The samples were mixed well and incubated at room temperature for another 3 min, followed by centrifugation. The upper aqueous phase was transferred to a new tube to which 500 µl of isopropanol was added, followed by a 10 min incubation at room temperature and centrifugation for 15 min at maximum speed. The pellet was washed with 75% (v/v) ethanol and finally dissolved in 100 µl H_2O. RNA samples for RNA sequencing were additionally purified on NucleoSpin RNA II columns (Machery-Nagel) according to manufacturer's instructions. RNA quantity and quality were determined using a Nanodrop ND1000 spectrophotometer.

RNA sequencing analysis

RNA sequencing was outsourced to ServiceXS (Leiden, The Netherlands). cDNA library constructions were performed using the Illumina mRNA-Seq Sample preparation kit according to the instructions of the supplier. In brief, mRNA was isolated from total RNA using oligo-dT magnetic beads. After fragmentation of the mRNA, cDNA synthesis was performed and the cDNA was ligated with the sequencing adapters before PCR amplification of the resulting product. The quality and yield after sample preparation were measured with a DNA 1000 Lab-on-a-Chip. Clustering and mRNA sequencing using the Illumina cBot and HiSeq 2000 were performed according to the manufacturer's protocol. For each RNA sample at least 3.2 Gb of sequence data were obtained that passed the quality control (% ≥ Q30). Image analysis, base calling and quality checks were performed

with the Illumina data analysis pipeline RTA v1.13.48 and/or OLBv1.9 and CASAVA v1.8.2. Quality-filtered sequence tags are available upon request.

Transcriptomic data analysis

RNA sequencing analysis was performed essentially as described previously (Wang *et al.*, 2015) except for the transfer of genome annotations. Annotations were transferred from the CBS 513.88 genome to the N402 genome based on bidirectional alignments created with LAST (version 417) (Kiełbasa *et al.*, 2011), with tandem repeat sections masked with TRF (Benson, 1999). Alignments were combined and chained using CLASP (Otto *et al.*, 2011). Gaps in the global alignment were improved by performing realignment using either LAST (for large gaps, in sensitive mode) or Needleman-Wunsch (for smaller gaps). Chains with scores > 150 were accepted for alignment transfer. In total, 13412 (of 14070) genes were transferred. The normalized, RNAseq-based expression data are summarized in Supplemental Table S1.

Annotation enrichment analyses

Overrepresented Gene Ontology (GO) terms in sets of differentially expressed genes (FDR q-value < 0.005) were determined by using the Fisher's exact test Gene Ontology tool FetGOat (Nitsche *et al.*, 2011). R statistical computing software (R Foundation for statistical computing) was used to perform k-means clustering analysis. Normalized fragment counts were transformed to log space using log2(fragment count + 16) and standardized (mean = 0 and standard deviation = 1). The optimal number of clusters was determined from a total within-cluster sum of squares plot and standardized gene expression values were subsequently clustered accordingly.

Results

Comparison of the transcriptomic response to submerged carbon starvation of *A. niger* wild-type and Δ*atg1* strains

Autophagy is one of the most dominantly induced processes during carbon starvation in *A. niger* (Nitsche *et al.*, 2012). In a previous study, we examined the effects of deleting genes essential for autophagy during carbon starvation and showed that growth profiles of wild-type and *atg* mutants were comparable yielding similar amounts of dry biomass (Nitsche *et al.*, 2013). However, the accelarated formation of carbon starvation-induced thin hyphae and earlier cell death of old hyphae suggested a role for autophagy in controlling cell cycle progression and cellular maintenance during starvation. To gain more insights in the cellular processes in cells defective for autophagy during carbon starvation, transcriptome changes were analyzed using paired-end mRNA sequencing analysis. Total RNA was extracted from biomass samples harvested from batch cultures of both wild-type and Δ*atg1* mutant strains

during the exponential growth phase and during carbon starvation. In order to compare the exponential phase with early and later stages of carbon starvation, three different time points during carbon starvation were assessed: 20 hours (day 1), 70 hours (day 3) and 140 hours (day 6) post carbon depletion. As shown in Figure 1 growth profiles of wildtype and Δ*atg1* mutant strains were very similar. Differentially expressed genes between wild-type and Δ*atg1* strains were identified applying a critical FDR q-value of 0.005, resulting in a total of 2815 genes that were found to be differentially expressed during at least one of the four time points (Table S1). During the exponential growth phase, only small sets of genes were either higher or lower expressed in the Δ*atg1* mutant compared to the wild-type (121 and 25 genes, respectively) and a majority of them showed higher or lower expression only during the exponential phase (69% and 68% respectively). Considering the post-exponential starvation phase, 238 genes were conjointly higher expressed in the Δ*atg1* mutant, while 118 genes were conjointly lower expressed during all three starvation time points (Figure 2). The number of differentially expressed genes shared between day 3 and day 6 was even higher (401 and 206 genes higher and lower expressed, respectively), in contrast to relatively low overlaps of genes between day 1 and day 3, and day 1 and day 6. This indicates that the differences in gene expression between wild-type and Δ*atg1*

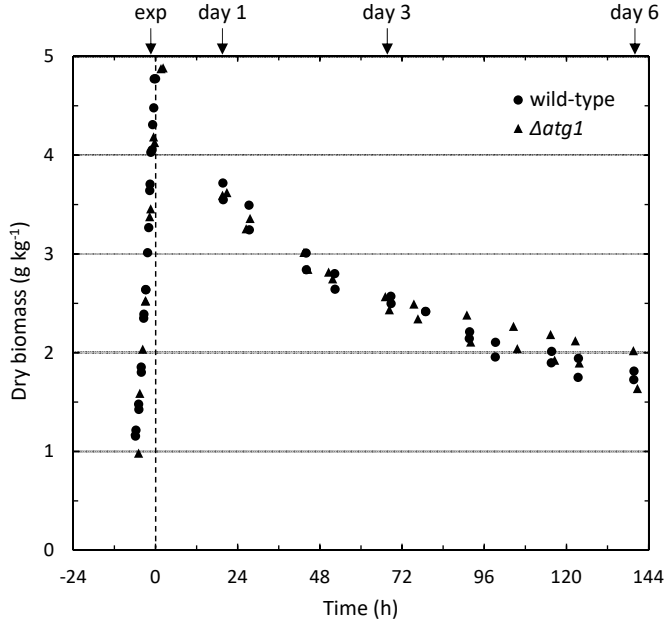

Figure 1 | Growth curves of duplicate submerged batch cultures of *A. niger* wild-type (N402) and Δ*atg1* strains. Replicate cultures were synchronized by setting the carbon depletion time points to 0. RNA was extracted from biomass samples taken during the exponential growth phase (exp) and 20 hours (day 1), 70 hours (day 3) and 140 hours (day 6) post carbon depletion, as indicated by arrows.

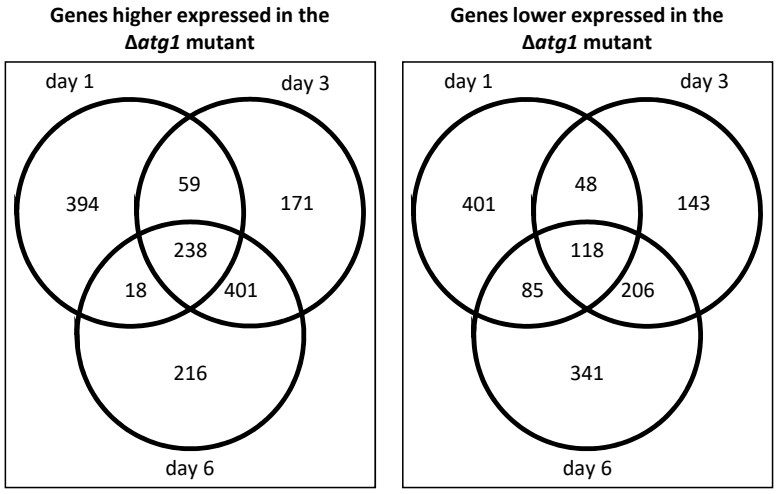

Figure 2 | Venn diagrams showing genes differentially expressed in the Δ*atg1* strain compared to the wild-type. Numbers of genes that are significantly higher (left) or lower (right) expressed in the Δ*atg1* strain compared to the wild-type during submerged carbon starvation. Differential expression (FDR q-value < 0.005) was determined during the exponential growth phase and at 1 day, 3 days and 6 days post carbon depletion. Numbers of differentially expressed genes during the exponential phase are not included in the figure for clarity reasons.

mutant are specific for the duration of carbon depletion, which is in accordance with the finding of distinct early and late carbon starvation responses in *A. niger* (Nitsche *et al.*, 2012). Subsequently, enrichment analysis was performed to identify overrepresented bioprocesses among the gene sets using the Gene Ontology tool FetGOat (Nitsche *et al.*, 2011). A summary of the results is shown in Figure 3 (see Table S2 for complete GO enrichment results). Remarkably, enriched GO-terms among differentially higher expressed genes in the Δ*atg1* mutant compared to the wild-type were identified during the exponential phase (although not more than one GO-term was found) and on day 1, but not on day 3 and day 6. Considering gene sets differentially lower expressed in the Δ*atg1* mutant compared to the wild-type, overrepresentation of GO-terms could be found on all starvation time points, but not during the exponential growth phase.

The early carbon starvation response: higher expression of cell division and DNA repair processes in the Δ*atg1* mutant

In order to deduce biologically relevant information from the GO enrichment analysis, we first focused on the set of enriched GO-terms identified from genes higher expressed in the Δ*atg1* mutant on day 1. Investigation of the GO-terms in this set of 709 genes (394 + 59 + 238 + 18) revealed that all of them could be subdivided into two main categories: cell division and DNA repair (Figure 3), indicating that genes related to cell division and DNA repair are higher expressed in the Δ*atg1* mutant compared to the wild-type during early carbon starvation. The corresponding genes, which are listed in Table 1, include orthologues

GO enrichment results for genes higher expressed in the Δ*atg1* mutant					
Exp	Day 1	Day 3	Day 6	GO-term	Description
Specific					
●				GO:0006083	acetate metabolic process
	●			GO:0000726	non-recombinational repair
	●			GO:0000727	double-strand break repair via break-induced replication
	●			GO:0006302	double-strand break repair
	●			GO:0010695	regulation of spindle pole body separation
	●			GO:0032465	regulation of cytokinesis
	●			GO:0042148	strand invasion
	●			GO:0045787	positive regulation of cell cycle
	●			GO:0090068	positive regulation of cell cycle process

GO enrichment results for genes lower expressed in the Δ*atg1* mutant					
Exp	Day 1	Day 3	Day 6	GO-term	Description
Common					
	●	●	●	GO:0000462	maturation of SSU-rRNA from tricistronic rRNA transcript (SSU-rRNA, 5.8S rRNA, LSU-rRNA)
	●	●		GO:0042273	ribosomal large subunit biogenesis
		●	●	GO:0000027	ribosomal large subunit assembly
		●	●	GO:0000028	ribosomal small subunit assembly
		●	●	GO:0006407	rRNA export from nucleus
Specific					
	●			GO:0019388	galactose catabolic process
		●		GO:0006412	translation
		●		GO:0006525	arginine metabolic process
		●		GO:0044238	primary metabolic process
			●	GO:0005980	glycogen catabolic process
			●	GO:0005982	starch metabolic process
			●	GO:0005996	monosaccharide metabolic process

Figure 3 | Summary of the GO enrichment results. GO enrichment analysis was performed with sets of genes differentially expressed (FDR q-value < 0.005) between wild-type and Δ*atg1* during the exponential growth phase as well as 1, 3, and 6 days post carbon depletion. Dots indicate common most-specific bioprocesses that are statistically significant overrepresented (FDR < 0.05) within a gene set.

of the *A. nidulans* cell cycle regulator genes *nimA, nimE* and *nimX* (An12g08100, An01g07420 and An11g02960, respectively) (Ye *et al.*, 1999) as well as the ku70 and ku80 orthologues *kusA* and *kueA* (An15g02700 and An07g05980) involved in non-homologous end-joining. It is important to note that the observed higher expression of genes involved in cell-division and DNA repair in the Δ*atg*1 mutant on day 1 does not allow conclusions about the mutant-specific response of these genes to early carbon starvation. More detailed examination of the expression values of the corresponding genes showed that only a minority of the genes (25%) was lower expressed in the wild-type and higher expressed in the Δ*atg1* mutant when comparing day 1 of the post-exponential phase with the exponential phase (Table

1). For a majority of the genes an increase or decrease in expression at day 1 compared to the exponential phase was found simultaneously in both wild-type and Δ*atg1* mutant, indicating that the observed significant differential expression resulted mostly from a difference in magnitude of the response to early carbon starvation. Both cell division and DNA repair processes were generally lower expressed upon carbon starvation in both strains as determined from lower expression values of corresponding genes at day 1 compared to the exponential phase, but the decrease was found to be less in the Δ*atg1* mutant compared to the wild-type. Analysis of the individual expression values further confirmed that the significant difference between wild-type and *atg1* deletion mutant considering cell division and DNA repair processes was specific to early carbon starvation only, as from the corresponding genes that were significantly higher expressed in the Δ*atg1* mutant at day 1, only 21% was found to be also significantly higher at day 3 and/or day 6 (Table 1). Also given the fact that both strains show identical growth curves (Figure 1), the results indicate that during early carbon starvation genes related to cell division and DNA repair are decreased in expression to a lesser extent in the Δ*atg1* mutant than in the wild-type, suggesting that these processes remain more active in the mutant during the early post-exponential phase.

Bioprocesses related to ribosomal function are lower expressed in the Δ*atg1* mutant during the post-exponential phase

During the exponential growth phase, only 25 genes were lower expressed in the Δ*atg1* mutant compared to the wild-type. Most likely as a result of this low number of genes, no overrepresented GO-terms were found in GO-enrichment analysis. In contrast, significant overrepresentation of a total of 49 unique bioprocesses was found among the genes lower expressed in the Δ*atg1* mutant compared to the wild-type during the post-exponential phase. As shown in Figure 3, GO-terms analysis revealed that both common as well as time point specific overrepresented GO-terms were identified among the genes lower expressed in the Δ*atg1* mutant. Bioprocesses related to ribosome biogenesis and assembly were enriched during all starvation time points, suggesting that ribosomal function might be decreased in the Δ*atg1* mutant during carbon starvation possibly as a result of less available building blocks for protein synthesis.

To investigate and compare the response to starvation of the corresponding ribosomal genes (n = 100) both in the wild-type and in the autophagy deletion mutant, individual gene expression profiles were assessed. Based on the expression profiles at all different time points, the genes were assigned to three different clusters by applying K-means clustering analysis to standardized expression values. The resulting clusters contained unequal number of genes (Figure 4) and the distribution of the genes over the clusters could not be related to functional nor genomic clustering (data not shown). The results show that 92 out of 100 genes were assigned to clusters 1 and 2, which contain genes with lower expression

Table 1 | Transcriptome data of genes corresponding to bioprocesses that are enriched among higher expressed genes in the Δatg1 mutant at day 1.

		Fold change Δ*atg1*/WT[a,b]				Fold change day 1/exp	
Identifier	**Description**	**Exp[c]**	**Day 1**	**Day 3**	**Day 6**	**WT**	**Δ*atg1***
Cell division							
An01g03090	strong similarity to 1,3-beta-glucanosyltransferase *gel1*–*A. fumigatus*	0.9	2.5	3.0	2.4	21.5	58.4
An02g11920	strong similarity to fizzy-related protein Fzr1–*Mus musculus*	1.0	2.1	2.2	1.6	1.6	3.7
An12g08530	similarity to Swe1 regulating protein kinase Hsl1–*S. cerevisiae* [truncated ORF]	0.9	2.5	0.8	0.5	1.1	2.9
An08g10320	strong similarity to checkpoint protein kinase chk1p–*Schizosaccharomyces pombe*	1.1	2.4	2.3	2.1	0.8	1.7
An11g11100	strong similarity to cell cycle protein kinase hsk1p–*S. pombe*	1.0	1.7	1.2	0.9	0.6	1.0
An01g07420	strong similarity to cyclin B *nimE*–*A. nidulans*	1.0	2.0	0.8	0.8	0.4	0.7
An01g12750	strong similarity to cell cycle protein CDC20–*Homo sapiens*	1.0	2.4	0.8	0.6	0.3	0.7
An05g00100	strong similarity to aurora/IPL1-related kinase AIK–*H. sapiens*	1.1	2.2	0.7	0.6	0.3	0.6
An05g00280	similarity to protein kinase Swe1–*S. cerevisiae*	1.0	1.8	0.8	0.9	0.4	0.8
An07g08210	strong similarity to cytoskeleton regulator IQGAP1–*H. sapiens*	0.9	2.1	0.9	0.7	0.4	0.8
An09g05760	similarity to hypothetical protein SPAC9G1.06c–*S. pombe*	1.0	1.8	1.2	1.3	0.3	0.5
An09g06400	Glycosylphosphatidylinositol-anchored chitinase *ctcA*–*A. niger*	1.0	6.8	3.9	2.2	0.1	0.9
An11g02000	strong similarity to spindle assembly checkpoint protein SldA–*A. nidulans*	1.0	2.0	0.7	0.5	0.4	0.8
An11g02960	strong similarity to protein kinase functional homolog of cdc2 NimX–*A. nidulans*	1.0	1.8	0.9	0.7	0.3	0.6
An12g08100	strong similarity to serine/threonine protein kinase NimA–*A. nidulans*	1.1	2.3	1.1	1.0	0.4	0.9
An14g00660	strong similarity to chitin synthase *chsA*–*A. nidulans*	1.1	2.3	0.9	0.7	0.4	0.8
An14g05530	Rho GTPase *rhoD*–*A. niger*	1.0	3.3	0.9	0.7	0.2	0.6
An16g07040	similarity to beta-1,3-glucanosyltransferase *bgt1*–*A. fumigatus* [truncated ORF]	1.0	2.3	0.7	0.9	0.3	0.8
DNA repair							
An07g05980	Ku80 ortholog involved in non-homologous end-joining *kueA*–*A. niger*	1.3	1.8	1.7	1.3	1.1	1.6
An01g05260	strong similarity to DEAH protein Mph1–*S. cerevisiae*	1.0	1.9	0.8	0.7	0.6	1.2
An03g02640	strong similarity to DNA ligase CaLIG4–*Candida albicans* [putative frameshift]	1.2	2.0	2.1	1.7	0.8	1.4
An04g01290	strong similarity to Rad52 homologue MUS11–*Neurospora crassa* [truncated ORF]	1.2	2.4	1.4	1.2	0.7	1.4

Continue

Continued

Identifier	Description	Fold change Δ*atg1*/WT[a,b]				Fold change day 1/exp	
		Exp[c]	Day 1	Day 3	Day 6	WT	Δ*atg1*
An07g08490	similarity to ATP-dependent helicase pcrA–*Bacillus stearothermophilus*	1.2	2.3	1.4	0.8	0.9	1.7
An15g02700	Ku70 ortholog involved in non-homologous end-joining kusA–*A. niger*	1.2	1.9	1.2	1.0	0.7	1.1
An01g13280	strong similarity to RAD54B – *H. sapiens*	1.3	1.9	1.2	0.8	0.3	0.5
An08g02350	strong similarity to protein uvsC–*A. nidulans*	1.2	1.9	1.0	0.8	0.4	0.6
An08g02440	similarity to DNA polymerase lambda POL lambda–*H. sapiens*	1.2	1.9	1.3	1.4	0.5	0.8
An08g10560	strong similarity to Rad54 homolog mus-25–*N. crassa*	1.1	1.8	1.3	1.4	0.4	0.7

[a] Significant differentially expressed genes are shaded in grey (FDR q-value < 0.005)
[b] WT, wild-type
[c] Exp, exponential growth phase

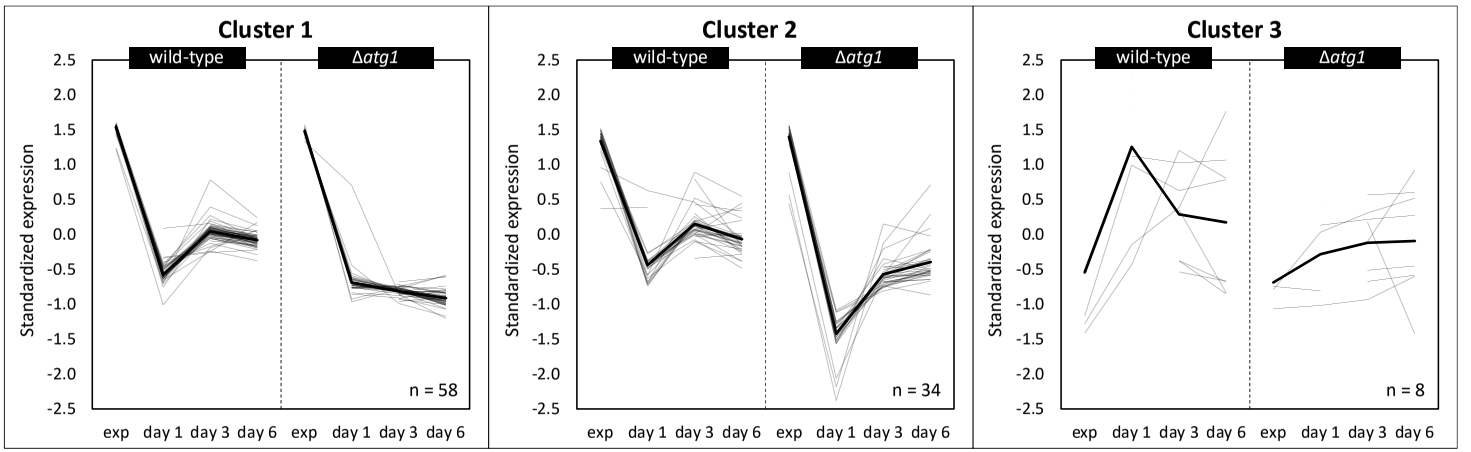

Figure 4 | Clustering of gene expression profiles for a subset of genes related to ribosomal function. The k-means clustering analysis was performed with a total of 100 genes, which were identified from GO enrichment analyses among genes that are lower expressed in the Δ*atg1* mutant during carbon starvation. Enriched GO-terms related to ribosomal processes were selected and the corresponding genes were used for clustering analysis. Normalized fragment counts were transformed to log space, standardized and subsequently clustered. Bold lines indicate mean expression profiles per cluster.

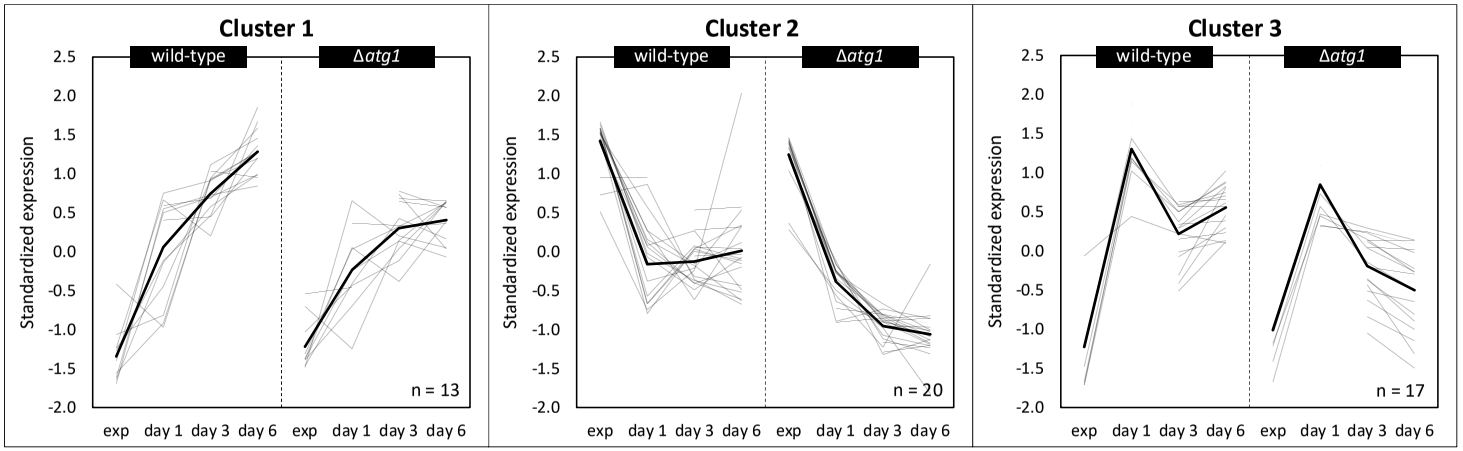

Figure 5 | Clustering of gene expression profiles for a subset of genes related to catabolic and metabolic bioprocesses as identified from GO enrichment results. From the GO enrichment analyses among lower expressed genes in the Δ*atg1* mutant during carbon starvation, overrepresented bioprocesses related to catabolism and metabolism were selected and the corresponding genes (n = 50) were used for k-means clustering analysis. Normalized fragment counts were transformed to log space, standardized and subsequently clustered. Bold lines indicate mean expression profiles per cluster.

values during carbon starvation compared to the exponential growth phase. For a vast majority of the genes (89 in the wild-type and 92 in the Δ*atg1* mutant) this downregulation was significant during at least one of the starvation time points with an FDR q-value below 0.005. The difference between cluster 1 and cluster 2 was determined by the Δ*atg1* gene expression profiles as gene expression profiles for the wild-type were similar between cluster 1 and cluster 2. The autophagy mutant expression profiles showed an initial decrease in gene expression upon starvation in both clusters, followed by increasing expression in cluster 1 and a decrease in expression in cluster 2. The third cluster contains the remaining eight genes. Significant upregulation for at least one of the starvation time points was observed for 7% and 3% of the genes in the gene set in wild-type and mutant, respectively. Starvation-induced upregulation of a gene in the wild-type and downregulation in the mutant at the same time point in the post-exponential phase was also observed from the expression profiles, but never significant. Taken together, the gene expression profiles and differential expression analysis show that ribosomal genes are generally significantly downregulated upon carbon starvation. Furthermore, increases and decreases in ribosomal gene expression mostly happen simultaneously in wild-type and *atg1* mutant, but the magnitude of the response is different. As autophagy plays an important role in cellular maintenance during starvation by the recycling of cellular products to be reused by the cell, lower expression of genes related to ribosome function in the autophagy mutant could be the consequence of lower availability of building blocks. This implicates that the cell is less capable to adapt to carbon starvation conditions by efficient turnover of macromolecules, which is in agreement with our previous observation that cell death of older hyphae is accelerated in autophagy mutants (Nitsche *et al.*, 2013).

The late carbon starvation response: lower expression of metabolic processes in the Δ*atg1* mutant

The majority of the overrepresented GO-terms identified from lower expressed genes during the post-exponential phase in the *Δatg1* mutant was related to protein synthesis and was commonly found on all three starvation time points. In addition, enrichment analysis also identified time-dependent responses specific to early, intermediate and late carbon starvation (Figure 3). Most of them were related to certain metabolic processes e.g. galactose catabolic process (day 1), arginine metabolic process (day 3), glycogen catabolic process, starch and monosaccharide metabolic processes (day 6). None of the identified metabolic pathways showed overlap between the time points. Investigation of the expression values of genes corresponding to the enriched GO-terms revealed that the vast majority of the genes was lower expressed in the Δ*atg1* mutant for all starvation time points, and especially for day 3 and day 6. However, as this was mostly not significant, no conclusions can be drawn for specific metabolic pathways on time points different than resulting from the enrichment analysis.

During late carbon starvation (120h post carbon depletion, day 6) multiple metabolic and catabolic processes were lower expressed in the Δ*atg1* mutant (Figure 3). The set of genes corresponding to these particular bioprocesses identified on day 6 consisted of 50 unique genes. K-means clustering analysis performed with this gene set resulted in three distinct clusters showing similar profiles of gene expression during the exponential phase and during carbon starvation (Figure 5). Clusters 1 and 2 consisted of genes that show respectively an increase or a decrease in gene expression during all starvation time points compared to the exponential phase, whereas genes in cluster 3 showed an increase in gene expression during the early post-exponential phase (day 1) followed by a decrease in expression during later starvation time points (day 3 and day 6). All bioprocesses were represented in all three clusters, except for GO:0005980 (glycogen catabolic process) and GO:0005982 (starch metabolic process). Enriched genes corresponding to these two particular GO-terms were found in clusters 2 and 3, but not in cluster 1 (data not shown). Among the genes related to starch metabolism were the members of the amylolytic cluster (*amyR-agdA-amyC*), which were all assigned to cluster 2 showing decreasing expression values following carbon starvation.

Discussion

The transcriptomic profiling of *A. niger* wild-type and Δ*atg1* strains during submerged carbon starvation uncovered significant differences approving that autophagy plays an important role specifically during these conditions. The data showed that during the exponential growth phase only small sets of genes were differential expressed between the wild-type and the mutant. This is in accordance with our previous study, in which we demonstrated that for autophagy mutants only a mild reduction in growth rate could be observed both in surface and in submerged growth, while no morphological differences were seen during exponential growth (Nitsche *et al.*, 2013).

During early starvation (20 hours after glucose depletion) bioprocesses related to cell cycle regulation and DNA repair were significantly higher expressed in the Δ*atg1* mutant compared to the wild-type (Table 1). This suggests a higher cell division rate in autophagy mutants, which might increase the need for DNA repair mechanisms. It has been shown that TOR-mediated autophagy is involved (albeit not required) in cell cycle arrest awaiting the repair of severe DNA damage (Klermund *et al.*, 2014). Alternatively, the higher expression of genes related to DNA repair mechanisms could be resulting from the absence of autophagic mechanisms resolving DNA damage, consequently inducing other DNA repair pathways. Evidence for the involvement of autophagy in genome stability mainly results from studies in yeast and mammalian cells showing that autophagy has a strong impact in multiple ways. First of all, autophagy plays a role in mitigating DNA damage by controlling the

production of hazardous reactive oxygen species (ROS) through the degradation of injured mitochondria (Nitsche *et al.*, 2013; Kanki *et al.*, 2015). Secondly, autophagy can influence the dynamics of DNA repair by recycling key proteins involved in these mechanisms (Dyavaiah *et al.*, 2011; Robert *et al.*, 2011). Finally, autophagy contributes to the maintenance of nuclear function and genome stability by degrading damaged nuclei or nuclear components (Park *et al.*, 2009; Shoji *et al.*, 2010; Kikuma *et al.*, 2017a). Compromising the autophagy pathway during nutrient-limited conditions resulted in e.g. impaired mitochondrial turnover, aberrant nuclear division, increased DNA damage and aneuploidy (Mathew *et al.*, 2007; Matsui *et al.*, 2013; Nitsche *et al.*, 2013). But although a number of studies have demonstrated a link between autophagy and DNA integrity, its role is far from understood, as it can either contribute to or prevent cell death.

The expression of genes related to ribosome biogenesis and ribosome assembly was significantly lower in the Δ*atg*1 mutant on all starvation time points, whereas catabolic and metabolic processes were lower expressed specifically during the late post-exponential phase. Taking into account the importance of autophagy in the recycling of nutrients, this suggests that the level of metabolism is lower in the mutant as a consequence of a shortage for available building blocks. As an important catabolic program being required for maintaining cellular nutrient homeostasis, autophagy has been described to be involved in amino acid and lipid metabolism as well as in glycogen breakdown (Onodera and Ohsumi, 2005; Deng and Naqvi, 2010; Ha *et al.*, 2015; Müller *et al.*, 2015). It has been reported that *atg5* knockout mice have reduced amino acid concentrations in plasma and tissue during nutrient limitations in their early neonatal state (Kuma *et al.*, 2004), while an even more dramatic reduction in free amino acid pools was observed in Δ*atg7* yeast cells (Onodera and Ohsumi, 2005). Furthermore, consistent with its key role in amino acid recycling, autophagy-deficient *S. cerevisiae* Δ*atg7* and Δ*atg8* mutants showed decreased levels of protein synthesis compared to wild-type cells during nitrogen starvation (Onodera and Ohsumi, 2005; Müller *et al.*, 2015). In this respect it is interesting to note that the non-classically secreted protease, PepN (An01g00370) and a presumably non-classical secreted hemolysin (An19g00210) were overexpressed in the Δ*atg1* mutant at all time points respectively in the exponential phase (Table S1), corroborating our earlier finding that non-classical protein secretion is not decreased in *atg* deletion mutants (Burggraaf *et al.*, 2016). Although a role of autophagy in secondary metabolism was not clearly identified, it is also interesting to note that the fumonisin biosynthetic gene cluster (An01g06820-An01g06930) was highly overexpressed in the Δ*atg1* mutant during the exponential phase (Table S1). Another gene cluster, with amylolytic genes (An04g06910-An04g06930) showed decreased expression upon carbon starvation with significant lower expression values in the Δ*atg1* mutant as compared to the wild-type during starvation. In addition, significant lower expression in the autophagy deletion mutant was also observed for acid α-amylase (*aamA*) and glucoamylase (*glaA*). These particular amylolytic genes have been associated

with repression under secretion stress (RESS), a mechanism activated during secretion stress which selectively downregulates genes encoding secreted proteins (Al-Sheikh *et al.*, 2004; Guillemette *et al.*, 2007; Carvalho *et al.*, 2012). Hence, lower expression of these genes in the Δ*atg1* mutant might indicate that secretion stress is elevated in the absence of functional autophagy. However, the ER stress marker genes *bipA* and *pdiA* were not significantly higher expressed in the Δ*atg1* mutant compared to the wild-type (Table S1). Furthermore, it has been demonstrated that ER-accumulation of the constitutively expressed misfolded mutant GlaA::GFP protein was not increased in the autophagy mutant background compared to the wild-type background (Burggraaf and Ram, 2016), indicating that ER stress levels were comparable between mutant and wild-type and the diminishing of ER stress via the degradation of misfolded proteins was independent of autophagy.

A. niger autophagy deletion mutants grown in carbon-starved submerged cultures showed accelerated cell death of older hyphal compartments accompanied by a faster emergence of thin, unbranched hyphae when compared to wild-type (Nitsche *et al.*, 2013). On the phenotypic level as well as from the transcriptome it becomes clear that autophagy plays an important role in the adaptation to nutrient-limited conditions by affecting multiple cellular processes. Our data suggest that autophagy is protective against cell death though the degradation of excessive or harmful cellular products (including ROS) while providing new building blocks supporting changes in metabolism and protein synthesis.